Internal Pulsed Valve Sample Introduction on a Quadrupole Ion Trap Mass Spectrometer

Brad I. Coopersmith* and Richard A. Yost

Department of Chemistry, University of Florida, Gainesville, Florida, USA

A pulsed valve positioned just outside the ion trap electrodes (within the vacuum chamber) has been characterized. The observed gas pulse widths and the maximum ion intensities were found to decrease as the distance between the pulsed valve and the ion trap electrodes increased. An explanation is presented within. The pulsed valve was found to impart temporal separation in ion–molecule reactions by permitting the removal of interfering neutrals. Other factors that affect the degree of temporal separation also are presented. *(J Am Soc Mass Spectrom 1995, 6, 976–980)*

Early work with gas-phase ion–molecule reactions focused on determination of the solvent effects by obtaining intrinsic information about chemical reactions [1–2]. Since then, gas-phase ion–molecule reactions have been designed to mimic their solution-phase counterparts. This methodology has been used previously to identify functional groups [3, 4], to distinguish between isomers [5–9], and to model biological activity [10–12].

The quadrupole ion trap mass spectrometer (QITMS) and the Fourier transform mass spectrometer (FTMS) are tandem-in-time instruments (they perform two or more stages of mass spectrometry sequentially in the same volume of space). This characteristic offers several advantages for the performance of ion–molecule reactions. Because the time of each stage of mass spectrometry can be controlled directly, both instruments can act as ideal gas-phase reaction chambers for kinetics studies. Also, the tandem-in-time nature permits multiple stages of mass spectrometry (MS^n, $n > 2$) to be performed, which enables the full characterization of product ions [13–18].

In our laboratory, investigations into the use of ion–molecule reactions between ionized nucleophiles (model DNA bases such as pyridine) and reactive electrophiles (potential carcinogens such as the allyl halides) for environmental monitoring have been initiated [10, 11]. In these reactions, the production of ionized nucleophile–reactive electrophile adduct ions is used to estimate the carcinogenicity of the electrophile. One drawback to the use of tandem-in-time instruments for ion–molecule reactions is the lack of spatial separation between the ions and neutrals, which can lead to unwanted and often unanticipated side reactions. In this case, reaction with the neutral nucleophiles can interfere with the detection of the reactive electrophiles.

One approach to minimize this interference is to introduce the neutral nucleophile through a pulsed valve. Pulsed valve introduction was first employed effectively on the FTMS for the momentary introduction of a high pressure of collision and reagent gases [19–22]. For these studies, the pulsed valve was located external to the FTMS high vacuum chamber and was connected either through an extension on a ConFlat cap [19, 22, 23] or through stainless steel tubing [20]. Due to the diffusional broadening of the gas pulse though the connective tubing and the large volume of the FTMS chamber that must be pumped, the observed gas pulses had long rise times (> 50 ms) and pulse widths [full width at half-maximum (FWHM) ≥ 100 ms] [20, 23]. To reduce the observed rise time and gas pulse width, pulsed valve introduction was employed on the smaller volume QITMS [5, 24]. Similar to the FTMS work, the pulsed valve was mounted externally to the ion trap vacuum chamber, connected directly to the ion trap via 1/16-in. stainless steel tubing [24]. The gas pulse width and rise time, determined by following the variation of the $N_2^{+\cdot}$ ion signal intensity as a function of time from the opening of the pulsed valve to introduce the N_2, were found to decrease as the connecting tubing was shortened; the shortest pulse width (FWHM ≈ 50 ms) and rise time (≈ 20 ms) used 2.5 cm of connecting tubing [24].

To effectively monitor potential carcinogens as they elute, several ion–molecule scans must be performed across a gas chromatography peak [25]. To minimize interferences from the reagent neutrals and to allow the fastest sampling rate possible, the gas pulse width must be as short as possible. Following the observed trend in the FTMS and in the QITMS, the shortest obtainable pulse width would occur for no connective tubing, which means that the pulsed valve would be

Address reprint requests to Dr. Richard A. Yost, Department of Chemistry, University of Florida, Gainesville, FL 32611-7200.

* Current address: Sandoz Pharmaceuticals, 59 Route 10, East Hanover, NJ 07936.

1044–0305/95/$9.50

SSDI 1044-0305(95)00528-I

Received February 23, 1995

Revised June 26, 1995

Accepted June 26, 1995

inside the vacuum chamber. This internal configuration will allow quick removal of the nucleophile neutrals by removing the diffusional broadening of the gas pulse caused by the tubing.

This communication presents initial results from an internally mounted pulsed valve. The factors that control the gas pulse width from this internal configuration are discussed. By minimizing interfering reactions between ionized pyridine and pyridine neutrals while maximizing reactions between the ionized pyridine and neutral allyl iodide, this internal pulsed valve configuration also is shown to implement temporal separation effectively into the ion–molecule reactions.

Experimental

All experiments were performed on a Finnigan-MAT (San Jose, CA) ion trap mass spectrometer (ITMS). All compounds were obtained from the manufacturer and used without further purification. Samples for the constant pressure studies were introduced through Granville-Phillips (Boulder, CO) Series 203 variable leak valves. The valves were heated to a constant temperature of 70 °C. All pressures reported were measured by a Bayard–Alpert ionization gauge mounted on the vacuum chamber and are uncorrected. Sample pressures ranged from 1×10^{-7} to 3×10^{-6} torr.

Pulsed valve introduction of the nucleophiles was through a Series 9 pulsed valve (General Valve Corp., Fairfield, NJ). An expanded view of the pulsed valve experimental setup is shown in Figure 1. The hardware consists of a pulsed valve mounted on 1/4-in. stainless steel tubing, which was inserted into the ITMS chamber through a 1/4-in. bored-through Cajon (Macedonia, OH) adapter welded to the flange. A Teflon sleeve, which contained two sets of relief holes, was used to act as a splitter for the pulsed sample. The Teflon sleeve was held in place by a stainless steel brace (not shown) mounted to the chamber flange. The exit orifice diameter of the pulsed valve was 0.006 in.

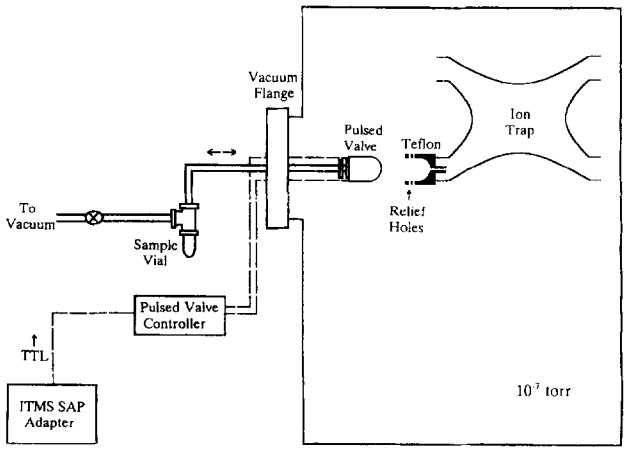

Figure 1. Schematic for internal pulsed valve introduction.

Ion catcher software, ICMS© (developed by Nathan A. Yates at the University of Florida), was used to allow software control of the TTL signal on the ITMS scan acquisition processor adapter board. This TTL signal triggered a pulsed valve controller built at the University of Florida. The duration of the control signal emitted from the pulsed valve controller was measured by a LeCroy (Chestnut Ridge, NY) 9400 dual channel 125-MHz digital oscilloscope.

The scan function used to perform the pulsed valve experiments is presented in Figure 2. A TTL trigger pulse (step A) was generated prior to ionization to introduce the pyridine (nucleophile N) neutrals through the pulsed valve. After an appropriate delay (step B) to reach the apex of the gas pulse, ionization (step C) at $q(N^{+\cdot}) = 0.23$ was followed by reagent ion formation (step D) and two-step rf/dc isolation (step E) [26, 27] of the pyridine molecular ion ($N^{+\cdot}$, m/z 79). After isolation, the pyridine molecular ions were allowed to react with both the pyridine and allyl iodide neutrals present inside the ion trap for up to 500 ms at $q(N^{+\cdot}) = 0.3$ (step F). Mass spectra were acquired with the axial modulation (530 kHz; 6 V_{p-p}) mass-selective instability scan (step G) [28].

Results and Discussion

Characterization of Pulsed Valve Introduction

Three major factors influenced the effectiveness of the pulsed valve when mounted inside the ITMS chamber: (1) the distance between the valve and the ion trap, (2) the length of the delay, ionization, and isolation times, and (3) the duration of the pulsed valve open period. The distance between the valve and the ion trap was found to affect the fraction of the sample pulse that entered the ion trap, the time necessary to reach the apex of the gas pulse, and the sample pulse width. Figure 3 presents the total ion intensity (measured as

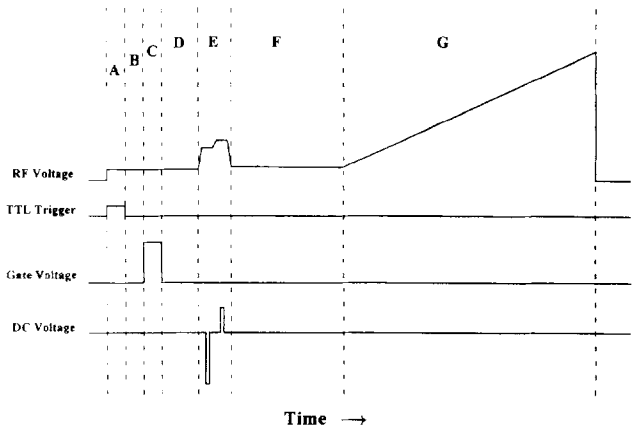

Figure 2. Scan function (not drawn to scale) used for pulsed valve introduction. Shown are valve open (A), delay time (B), ionization (C), reagent ion formation (D), reagent ion isolation (E), ion–molecule reaction time (F), and the mass-selective instability scan (G).

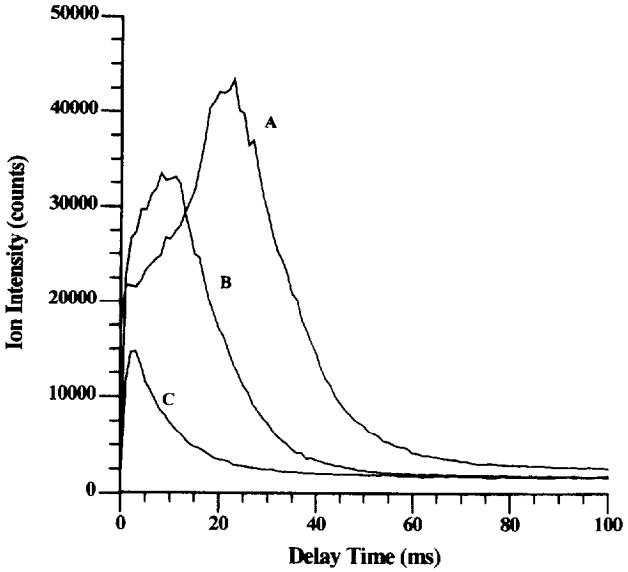

Figure 3. Effects of distance and delay time on observed pulse width. The distance between the pulsed valve and the QITMS is (A) 0-in., (B) 0.5-in., and (C) 0.75-in. The control pulse duration is 1.93 ms.

the reconstructed ion current from m/z 25 to 200) for pyridine as a function of both the distance between the valve and the ion trap and the time between the closing of the pulsed valve and ionization (referred to as the delay time) for a control pulse duration of 1.93 ms. Figure 1 shows that the Teflon sleeve into which the valve was positioned has two sets of relief holes. These relief holes act as a splitter for the pulsed sample. When the pulsed valve was positioned at the front of the sleeve, the valve orifice was located closest to the ion trap. Therefore, when the valve was opened, nearly all of the sample that was introduced went directly into the ion trap. Placing the pulsed valve at this location resulted in the largest neutral population inside the QITMS, as shown by curve A in Figure 3. When the pulsed valve was backed away from the ion trap, but still positioned inside the Teflon sleeve, enough space was created between the pulsed valve and the relief holes that some of the sample was split away. Part of the sample entered into the ion trap and the rest of the sample passed through the relief holes into the vacuum manifold. This split of the sample pulse lowered the ion intensities as shown by curve B in Figure 3. Curve C demonstrates that when the valve was withdrawn beyond the end of the Teflon sleeve, the greatest degree of splitting occurred.

Figure 3 also demonstrates that after the pulsed valve was closed, both the length of time needed to reach the apex of the sample pulse and the sample pulse width (FWHM) decreased as the distance between the valve and the ion trap increased. These trends are opposite to trends observed with the external pulsed valve [24]. This difference can be understood in terms of conductance or the rate at which the neutrals are introduced and removed from a given volume of space.

The overall rate of change of the number of neutrals is a function of both their rate of introduction and their rate of removal. This can be described as

$$\frac{d[\text{neutral}]}{dt} = \text{rate of introduction} - \text{rate of removal} \quad (1)$$

Integration of this equation with the appropriate functions for the rates of introduction and removal should produce a neutral pulse that increases logarithmically for a certain length of time and then decreases exponentially. The length of time that the curve increases is dependent upon (a) the difference in the rates of introduction and removal and (b) the length of time the valve is opened. For a given valve open time, the amount of sample introduced is constant due to the constant conductance of the pulsed valve. The rate of neutral removal, however, changes depending upon the position of the pulsed valve. When the pulsed valve is located at the front of the Teflon holder, the entire sample is introduced into the ion trap; therefore, the rate of removal is only due to the conductance of the ion trap. As the pulsed valve is backed away from the ion trap but still inside the Teflon holder, the rate of removal becomes a function of the conductance of both the ion trap and the relief holes of the Teflon holder. The conductance of the ion trap remains constant, but the conductance of the Teflon holder increases as the pulsed valve is displaced farther from the ion trap due to the incorporation of the relief holes.

As the rate of removal increases, two things will happen to the curve from eq 1. First, the time needed to reach the apex will shorten. Second, once the pulsed valve is closed, only the rate of removal matters. Therefore, with increasing conductance, the exponential decay will increase, which results in a steeper slope on the backside of the curve and a shorter pulse width. These trends are evident from both the positions of the sample pulse apexes and the corresponding sample pulse widths for curves B (20 ms at FWHM) and C (10 ms at FWHM) in Figure 3.

Recall that Figure 3 employs ion intensity as a measure of the number of neutrals in the trap. Note for instance the unusual shape of curve A for the first 25 ms. This shape is most likely due to saturation of the ion detection process, presumably due to space charge effects on ionization, ion storage, or ion detection. When the entire pulsed sample is introduced into the ion trap, as is the case for curve A, the number of ions formed at short delay times will be large enough to saturate ion detection and reduce the detected ion intensity. As the pyridine neutrals are pumped away with increased delay times, the extent of saturation decreases and the ion intensity increases. Eventually, enough neutrals are removed from the ion trap that

ion detection is no longer saturated. At this point, the ion intensity reaches a maximum and begins an exponential decay, as described earlier. Finally note also that a 1.93-ms control pulse opens the valve for less than 1.93 ms; indeed, control pulses of less than 1.5 ms do not open the valve at all.

Spectra Obtained from Internal Pulsed Valve Introduction

Figure 4a presents the product ion spectrum for the reaction between pyridine molecular ions ($N^{+\cdot}$) and allyl iodide (EX) and pyridine (N) neutrals. Detailed studies of these reactions [29] have shown that the product ions at m/z 120, the pyridine–allyl adduct ion (NE^+), and at m/z 206, the pyridine–iodide adduct ion (NX^+), were due to the reaction of ionized pyridine with neutral allyl iodide. The product ion at m/z 80, protonated pyridine (NH^+), was due to reaction of ionized pyridine with neutral pyridine. The final product ion at m/z 285, a dipyridinium iodide ion (N_2X^+), resulted from further reaction of the m/z 206 ion with neutral pyridine. An analysis of this system indicated that the rate constant for the reaction of ionized pyridine with neutral pyridine was almost twice as large as the rate constant for the reaction of ionized pyridine with neutral allyl iodide [29]. This favored reactivity of the ionized nucleophile toward nucleophile neutrals was observed for a series of nucleophiles and electrophiles examined at the same pressures.

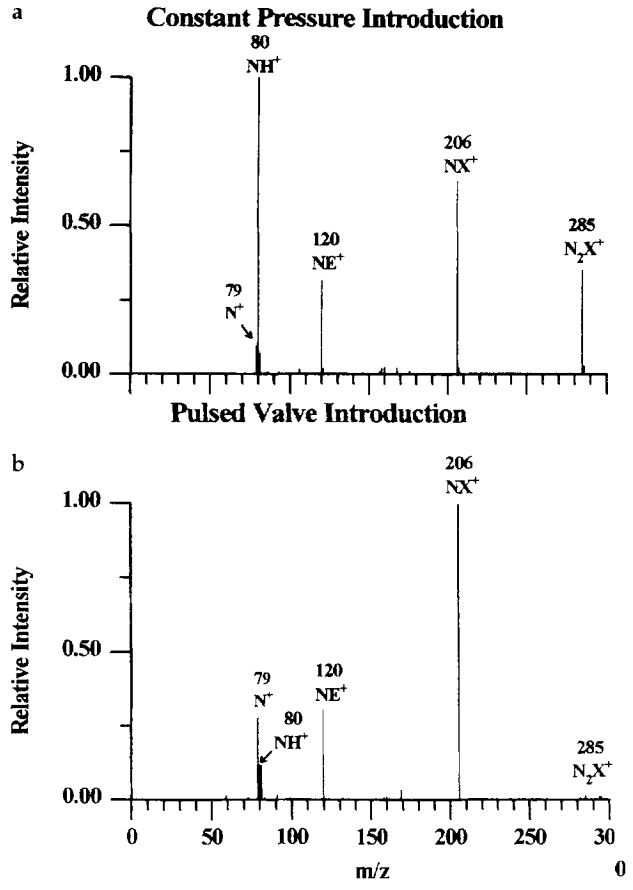

Figure 4. Product ion spectra for the 500-ms reaction of ionized pyridine with pyridine and allyl iodide neutrals. Allyl iodide is present at 5×10^{-7} torr for both spectra. (**a**) Pyridine introduced at constant pressure (5×10^{-7} torr); (**b**) pyridine introduced via pulsed valve introduction, with a pulsed valve open time of 1.65 ms and a delay time of 2 ms.

The product ion spectrum for pulsed valve introduction of pyridine with the same constant pressure (5×10^{-7} torr) of allyl iodide for 500 ms is shown in Figure 4b. In contrast to constant pressure introduction of pyridine (Figure 4a) in which protonated pyridine (NH^+) is the major product ion, pulsed valve introduction resulted primarily in the formation of the pyridine–iodine adduct ion (NX^+) at m/z 206 and the pyridine–allyl adduct ion (NE^+) at m/z 120. This product ion spectrum was due to the reaction of ionized pyridine almost entirely with the electrophilic allyl iodide neutrals. As expected, the use of pulsed valve introduction limited the extent of reaction with the neutral pyridine by significantly reducing its presence during the reaction period. However, the undesired side reactions were not totally eliminated, as evidenced by the slight formation of the protonated pyridine (NH^-) at m/z 80 and the dipyridinium iodine adduct ion (N_2X^+) at m/z 285. Because the reaction period was initiated when 80% of the neutral pyridine had been removed (an overall delay of 20 ms), there were still a small number of pyridine neutrals present to react.

Conclusions

Introduction of samples into the ion trap through a pulsed valve mounted inside the vacuum chamber has been presented. The diffusional broadening present when the pulsed valve is mounted outside the vacuum chamber has been eliminated. However, peak broadening still occurs and is a function of the conductance of the ion trap. As the pulsed valve is withdrawn from the ion trap, the conductance increases and the gas pulse width decreases. One consequence of displacement of the pulsed valve from the ion trap is that the amount of sample that enters into the ion trap volume decreases. Nevertheless, in most cases the amount of sample that enters into the ion trap volume should be more than sufficient to perform the desired experiments.

The main advantage to this configuration is the speed with which sample can be introduced and removed. Gas pulse widths (FWHM) of 10 ms were observed. This value could be reduced further with a shorter pulsed valve open time. The ability to rapidly pump away the nucleophile prior to the time period for ion–molecule reactions significantly reduces side reactions when potential carcinogens are monitored. Initial results from use of the internal pulsed valve

configuration for this purpose are promising and will be addressed in a subsequent publication.

Acknowledgments

The authors would like to thank the United States Environmental Protection Agency–ERL Duluth and the University of Florida Division of Sponsored Research for providing funding for this research.

References

1. Pellerite, M. J.; Brauman, J. I. *J. Am. Chem. Soc.* **1980**, *102*, 5993.
2. Tiedemann, P. W.; Riveros, J. M. *J. Am. Chem. Soc.* **1974**, *96*, 185.
3. Dolnikowski, G. D.; Allison, J.; Watson, J. T. *Org. Mass Spectrom.* **1990**, *25*, 119.
4. Eichmann, E. S.; Brodbelt, J. S. *J. Am. Soc. Mass Spectrom.* **1993**, *4*, 97.
5. Einhorn, J.; Kenttämaa, H. I.; Cooks, R. G. *J. Am. Soc. Mass Spectrom.* **1991**, *2*, 305.
6. Heath, T. G.; Allison, J.; Watson., J. T. *J. Am. Soc. Mass Spectrom.* **1991**, *2*, 270.
7. Kenttämaa, H. I.; Pachuta, R. R.; Rothwell, A. P.; Cooks, R. G. *J. Am. Chem. Soc.* **1989**, *111*, 1654.
8. Fetterolf, D. D.; Yost, R. A. *Int. J. Mass Spectrom. Ion Phys.* **1982**, *44*, 37.
9. Meyerhoffer, W. J.; Bursey, M. M. *Org. Mass Spectrom.* **1989**, *24*, 169.
10. Freeman, J. A.; Johnson, J. V.; Hail, M. E.; Yost, R. A.; Kuehl, D. W. *J. Am. Soc. Mass Spectrom.* **1990**, *1*, 110.
11. Freeman, J. A.; Johnson, J. V.; Yost, R. A.; Kuehl, D. W. *Anal. Chem.* **1994**, *66*, 1902.
12. Whitehill, A. B.; George, M.; Giblin, D.; Gross, M. L. *Proceedings of the 41st ASMS Conference Mass Spectrometry and Allied Topics*; San Francisco, CA, 1993; p 972a.
13. Marshall, A. G.; Grosshans, T. B. *Anal. Chem.* **1992**, *63*, 215A.
14. Beu, S. C.; Senko, M. W.; Quinn, J. P.; Wampler, F. M.; McLafferty, F. W. *J. Am. Soc. Mass Spectrom.* **1993**, *4*, 557.
15. Lay, J. O., Jr.; Gross, M. L. *J. Am. Chem. Soc.* **1983**, *105*, 3445.
16. Johnson, J. V.; Pedder, R. E.; Yost, R. A. *Int. J. Mass Spectrom. Ion Processes* **1991**, *106*, 197.
17. Louris, J. N.; Brodbelt-Lustig, J. S.; Cooks, R. G.; Glish, G. L.; Van Berkel, G. J.; McLuckey, S. A. *Int. J. Mass Spectrom. Ion Processes* **1990**, *96*, 117.
18. McLuckey, S. A.; Glish, G. L.; Van Berkel, G. J. *Int. J. Mass Spectrom. Ion Processes* **1991**, *106*, 213.
19. Carlin, T. J.; Freiser, B. S. *Anal. Chem.* **1983**, *55*, 571.
20. Sack, T. M.; Gross, M. L. *Anal. Chem.* **1983**, *55*, 2419.
21. Eller, K.; Schwarz, H. *Int. J. Mass Spectrom. Ion Processes* **1989**, *93*, 243.
22. Jacobson, D. B.; Freiser, B. S. *J. Am. Chem. Soc.* **1984**, *106*, 3891.
23. Hettich, R. L.; Jackson, T. C.; Stanko, E. M.; Freiser, B. S. *J. Am. Chem. Soc.* **1986**, *108*, 5086.
24. Emary, W. B.; Kaiser, R. E.; Kenttämaa, H. I.; Cooks, R. G. *J. Am. Soc. Mass Spectrom.* **1990**, *1*, 308.
25. Kleintop, B. L.; Yost, R. A.; Abolin, C. R. *J. Am. Soc. Mass Spectrom.* **1992**, *3*, 85.
26. Gronowska, J.; Paradisi, C.; Traldi, P.; Vettori, U. *Rapid Commun. Mass Spectrom.* **1990**, *4*, 306.
27. Yates, N. A., Yost, R. A.; Bradshaw, S. C.; Tucker, D. B. *Proceedings of the 39th ASMS Conference on Mass Spectrometry and Allied Topics*; Nashville, TN, 1991; p 1489.
28. Stafford, G. C.; Kelley, P. E.; Syka, J. E. P.; Reynolds, W. E.; Todd, J. F. J. *Int. J. Mass Spectrom. Ion Processes* **1984**, *60*, 85.
29. Coopersmith, B. I.; Yost, R. A.; Kuehl, D. W. *Proceedings of the 40th ASMS Conference on Mass Spectrometry and Allied Topics*; Washington, DC, 1992; p 180.